Lab on a Chip

Accepted Manuscript

This is an *Accepted Manuscript*, which has been through the Royal Society of Chemistry peer review process and has been accepted for publication.

Accepted Manuscripts are published online shortly after acceptance, before technical editing, formatting and proof reading. Using this free service, authors can make their results available to the community, in citable form, before we publish the edited article. We will replace this *Accepted Manuscript* with the edited and formatted *Advance Article* as soon as it is available.

You can find more information about *Accepted Manuscripts* in the **Information for Authors**.

ROYAL SOCIETY OF CHEMISTRY

www.rsc.org/loc

Acoustic Actuated Fluorescence Activated Sorting of Microparticles

Ola Jakobsson, Carl Grenvall, Maria Nordin, Mikael Evander, Thomas Laurell

Abstract

In this paper, we present a fluorescence activated sorter realized in a continuous flow microfluidic chip. Sorting is achieved by deflecting a focused particle stream with short acoustic bursts (2.5 ms), in a fluorescence activated configuration. The system utilizes two-dimensional acoustic pre-focusing , using a single actuation frequency, to position all particles in the same fluid velocity regime at flow rates up to 1.7 mL min^{-1}. Particles were sorted based on their fluorescence intensities at throughputs up to 150 particles s^{-1}. The highest purity reached was 80 % when sorting at an average rate of 50 particles s^{-1}. The average recovery of a sort was 93.2 ± 2.6 %. The presented system enables fluorescence activated cell sorting in a continuous flow microfluidic format that allows aseptic integration of downstream microfluidic functionalities, opening for medical and clinical applications.

Introduction

Background

The Fluorescence Activated Cell Sorter (FACS) remains a major workhorse in cell biology laboratories. After more than 40 years of development, the FACS excels at analyzing and sorting cells at very high speeds. Although throughput is an important factor, many applications involving cell sorting also put high demands on viability and require labor-intensive protocols both pre- and post-sorting. Exposure to high shear forces, from the hydrodynamic focusing and the droplet generation process, may affect cell viability[1]. The droplet based sorting mechanism in the conventional FACS complicates closed/aseptic system operation, which is needed when handling clinical or hazardous samples. By retaining sorted cells in a continuous flow throughout the sorting process, some of these limitations can potentially be overcome and additional functionality may be added in sequential downstream microfluidic unit operations.

Historically, a number of different FACS sorting mechanisms have been suggested, many of which are microchip based. Electro-osmotic [2], dielectrical [3], optical [4], and hydrodynamic forces [5] have been used to achieve fluorescence activated cell sorting in a continuous flow. The first FACS device based on the use of standing wave acoustic forces was presented by Johansson et al in 2009[6], utilizing the difference in fluid densities at a fluid-fluid interface to achieve deflection of particles. While many of these solutions demonstrate state-of-the-art technological solutions, they still suffer from limitations in terms of throughput [7], or require complicated fabrication protocols[8] in order to make them feasible for general cell sorting purposes.

An alternative approach to accomplish chip integrated cell sorting without any moving parts is to employ acoustophoresis, a technique based on standing wave acoustic forces that act directly on cells, in a fluorescence activated configuration. By actuating an acoustically resonant microfluidic structure with ultrasound at its resonance frequency, the resulting standing wave will induce an acoustic radiation force on cells and particles within this structure [9]. With proper design of the microfluidic structure it is possible to fabricate acoustofluidic components that enables focusing [10, 11],

enrichment [12], separation [13, 14], or gating of cells between multiple outlets[15, 16] in continuous flow based microsystems. An additional benefit of acoustophoretic cell handling is that it has been shown to be a gentle method for manipulation and sorting of cells [17,18]. Acoustophoresis is a non-invasive, robust and easy-to-use technique for manipulation of cells in suspensions. The uncomplicated design allows simple fabrication techniques to be used, opening a path towards low cost disposable Lab-on-a-chip devices.

In commercial FACS instruments, sheath flow is typically used to focus the sample into a very narrow stream prior to the laser interrogation point. The sample to sheath flow ratio typically ranges from 100:1 to 1000:1, diluting the sample during the analysis process. The sample flow rate for a commercial cytometer is typically limited to ranges between 30 and 120 µL min^{-1}. The hydrodynamic focusing is essential both for the analysis of the cells and the drop delay timing for the sorting process. Two-dimensional hydrodynamic focusing (sometimes also referred to as three-dimensional focusing in the literature), typically reserved for coaxial systems with large flow cells, can also be achieved in planar microchip systems using more elaborate fabrication techniques [19]. Other methods for achieving two-dimensional focusing in planar microchips includes hydrophoresis [20], inertia [21], dielectrophoresis [22] and "microfluidic drift focusing" [23, 24]. In previous work, Goddard et al. [25] have showed that acoustic focusing can be used to either eliminate or reduce the needs of hydrodynamic focusing for flow cytometry. While their work was done in coaxial capillary systems, the same principle can be applied to a rectangular micro-channels using a single [14] or multiple actuation frequencies [12, 26] in a planar format on-chip.

In this work, we present a microchip based FACS that is actuated with ultrasound as the sorting mechanism to achieve a binary sorting of particles based on fluorescence detection. Furthermore, the acoustic FACS described herein employs two-dimensional acoustic focusing, using a single actuation frequency. The acoustic actuated FACS (AFACS) can analyze and sort an event in the span of milliseconds, enabling chip integrated single cell sorting with relatively high throughput and purities.

Theory
Acoustophoresis

Acoustophoresis utilizes ultrasound standing waves to generate a force that acts on particles suspended in a medium. Acoustic actuation of the flow medium gives rise to a number of more or less complex acoustic force phenomena, out of which the primary acoustic radiation force, F_{rad}, dominates and can be used to explain the particle manipulation described in this paper (Eq. 1). By proper chip design this force can be utilized to position particles in a well-defined position in the flow channel cross-section.

The primary acoustic radiation force translates particles into acoustic pressure nodes or antinodes according to the acoustic contrast factor, Φ, of the particles (Eq. 2). The contrast factor is derived from differences in the density and compressibility of the particles and the surrounding medium. Dense particles (*i.e.* cells) have a positive contrast factor, and focus into the nodes when suspended in most commonly used media (water or PBS). In comparison, particles that are less dense than the medium will focus into the acoustic antinodes due to having a negative contrast factor. F_{rad} scales linearly with the contrast factor and the volume, a^3, of the particles.

$$F_{\text{rad}} = 4\pi a^3 \Phi k_y E_{\text{ac}} \sin(2 k_y y) \qquad \text{(1) Primary acoustic radiation force}$$

where

$$\Phi = \frac{\kappa_o - \kappa_p}{3\kappa_o} + \frac{\rho_p - \rho_o}{2\rho_p + \rho_o} \qquad \text{(2) Acoustic contrast factor}$$

and a is the particle radius, Φ is the acoustic contrast factor, $k_y = 2\pi / \lambda$ is the wave number, E_{ac} is the acoustic energy density, y is the distance from the wall, κ_p is the isothermal compressibility of the particle, κ_o is the isothermal compressibility of the fluid, ρ_p is the density of the particle and ρ_o is the density of the fluid.

Materials and methods

Fabrication of the microchip
The AFACS microfluidic chip was fabricated on a 400 μm thick 3 inch silicon wafer using conventional photolithography and wet etching protocols [10]. Wet etching of <100> silicon in KOH resulted in microfluidic-channels with a rectangular cross-section. Typically 12 chips could be fitted on one wafer. The chips were diced, anodically bonded to a 1.1 mm thick borosilicate glass lid, and fluidic ports were glued to the chip. Two piezoelectric ceramic plates, 1 mm and 400 μm thick respectively, (Pz26, Ferroperm Piezoceramics AS, Denmark) were attached to the microchip using cyanoacrylate glue. Silicon and glass was chosen as materials in favor of polymeric materials such as PDMS, due to their superior acoustic properties for acoustophoresis applications.

Acoustic Actuation
The two piezoelectric transducers were driven separately by two function generators (33120A, Agilent Technologies Inc., Santa Clara,CA, USA). The signal from the function generator that continuously actuated the "pre-focusing zone" with a 4.6 MHz sine wave was amplified with an in-house built circuit, based on a power amplifier (LT1012, Linear Technology Corp, Milpitas,CA, USA).

The function generator actuating the sorting zone with a 2 MHz sine wave was operating in "external triggered burst mode", meaning that upon a trigger signal, the sorting zone was actuated with a programmable number of periods, and then idle until the next trigger signal. The signal was amplified by the use of an amplifier (AR 75A250, Amplifier Research, Souderton, PA, USA). The function generator could not be retriggered unless a burst sequence was complete.

Optical detection and sorting trigger
A Photomultiplier Tube (PMT) (Photomultiplier tube R1617, Hamamatsu, Japan) was mounted in a fluorescence microscope (DM2500 M, Leica Microsystems CMS GmbH, Wetzlar, Germany) monitoring the desired area of the microchip (by adjusting pin hole and aperture settings). The signal from the PMT was coupled to a Schmitt trigger with adjustable threshold level and hysteresis. When a preset threshold level was exceeded, a 5 V TTL signal triggered the function generator, actuating the sorting zone. Both the PMT signal and the trigger signal were sampled by a data acquisition card (PCI-6024, National Instruments, Austin, TX, USA) and monitored in a computer environment (LabVIEW), recording the trigger event rate. A block diagram of the system is shown in Figure 1.
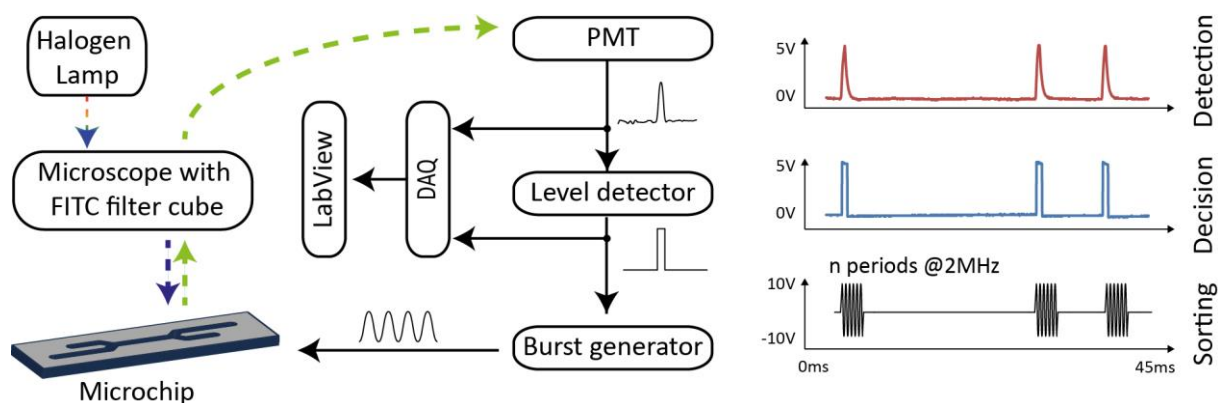
Figure 1. A block diagram of the optical system and sort trigger electronics. The signal from the PMT(red, top right) and the level detector (blue, middle right) are actual recordings. The signal from the burst generator (black, bottom right) is illustrated. Typically a burst contained between 5000-12000 periods at 2MHz.

Fluidics

Sample and sheath fluids were continuously infused through their respective inlets using syringe pumps (NeMESYS, Cetoni GMBH, Korbussen, Germany). The outflow ratio between the outlets was controlled by choosing tubing with different hydrodynamic resistance (diameter and length). The flow was split approximately at a 30:70 ratio between waste and target outlets. The samples from the target and waste outlets were collected in 15mL Falcon tubes.

Particle suspensions for sorting experiments

A suspension of 10 μm fluorescent particles (10 μm Melamine Resin FITC, Fluka/Sigma Aldrich, Buchs, Switzerland) and 10 μm non-fluorescent particles (10 μm Melamine Resin Plain, Fluka/Sigma Aldrich, Buchs, Switzerland) suspended in de-ionized water was prepared, and diluted to three samples with different concentrations. The concentration was matched to give a throughput of ~50, 100 and 150 particles s^{-1} at a flow rate of 200 μL min^{-1}. The purity of the samples was measured to 19.5 %.

Evaluating sorting purity

The purity of the samples before and after a sort was analyzed with a commercial flow cytometer (FACS Canto II with FACS Diva software, BD Biosciences, San Jose, CA, USA). The purity of a sample was defined as:

$$\text{Purity} = \frac{\text{number of fluorescent particles}}{\text{total number of particles}}$$

Aggregated beads (doublets and triplets) were excluded from the analysis to exclude non-system inherent bias. This gating did not affect the results significantly.

The recovery of target particles in the target outlet was estimated by analyzing the amount of target particles in the collected waste tube. The recovery was estimated by:

$$Recovery\ \% = 100 - \frac{purity\ waste\ outlet\ \%}{starting\ purity\ \%}$$

Confocal microscopy

Confocal microscopy was used to image the spatial distribution of microparticles in the micro-channel cross-section at the end of the pre-focusing zone of the microchip. FITC labeled fluorescent particles (10 µm FITC Polystyrene, Fluka/Sigma Aldrich, Buchs, Switzerland), suspended in de-ionized water, were used to obtain confocal images with an Olympus microscope (BX51WI, Olympus Corporation, Tokyo, Japan) and software (Fluoview 300) was subsequently used to reconstruct cross-section images.

Measuring particle velocity and retention time within the sorting zone

Particle velocity was measured by comparing particle positions between two subsequent frames. Images were recorded by using a microscope (DM2500 M, Leica Microsystems CMS GmbH, Wetzlar, Germany) mounted high frame rate CCD camera (EoSens mini MC-1370, Mikrotron GmbH, Unterschleissheim, Germany) and particle positions were determined using image analysis software (ImageJ). The length of the sorting zone was estimated to 1.7 mm. The retention time of a particle in the sorting zone was calculated by dividing this length with the average measured velocity for a given flow rate.

AFACS operating principle

Based on the acoustophoresis principle, we have developed an acoustically actuated FACS where short ultrasound bursts drive the sorting mechanism. The principle of the AFACS is illustrated in Figure 2. Particles are continuously injected into the chip through the sample inlet. A sheath fluid is injected through the sheath flow inlet, laminating the particle sample stream along the side wall. All particles are then two-dimensionally aligned in the "pre-focusing zone" by the acoustic radiation force. A piezoelectric transducer is continuously actuating the microfluidic channel at 4.6 MHz (one wavelength resonator), resulting in a standing wave with two horizontal pressure nodes, symmetrically placed on both sides of the channel centre, approximately 90 µm away from the walls respectively. The particles will, however, only reach and be forced into the horizontal pressure node closest to the sample side wall because of the sheath flow confinement to one side of the micro-channel. Due to the 2:1 aspect ratio of the channel, a vertical pressure node (½ wavelength resonator) will also form, which will force particles to the vertical center of the structure, hence providing two-dimensional focusing (simultaneous vertical and horizontal focusing) of the particles in the pre-focusing zone. This "pre-focusing step" improves the optical detection, sorting accuracy and throughput of the AFACS by aligning all particles in the same flow velocity vector.

After being precisely aligned in the "pre-focusing zone", the particles pass a "detection zone" before they reach the "sorting zone". The detection zone is monitored by a fluorescence filtered PMT which, upon detecting a fluorescent particle, sends a signal to an electronic system that triggers a sorting event. When a sorting decision is made, the sorting zone of the chip is actuated with a 2 MHz (½ wavelength resonator) ultrasonic burst, deflecting particles towards the horizontal center of the sorting zone, approximately 90 µm, which is sufficient to allow translation of these particles into the target outlet. The flow ratio between the waste and target outlets is approximately 30:70. The ultrasonic burst length is matched to the retention time of a particle in the sorting zone of the chip, thus achieving optimal system performance (see S1 of SI).
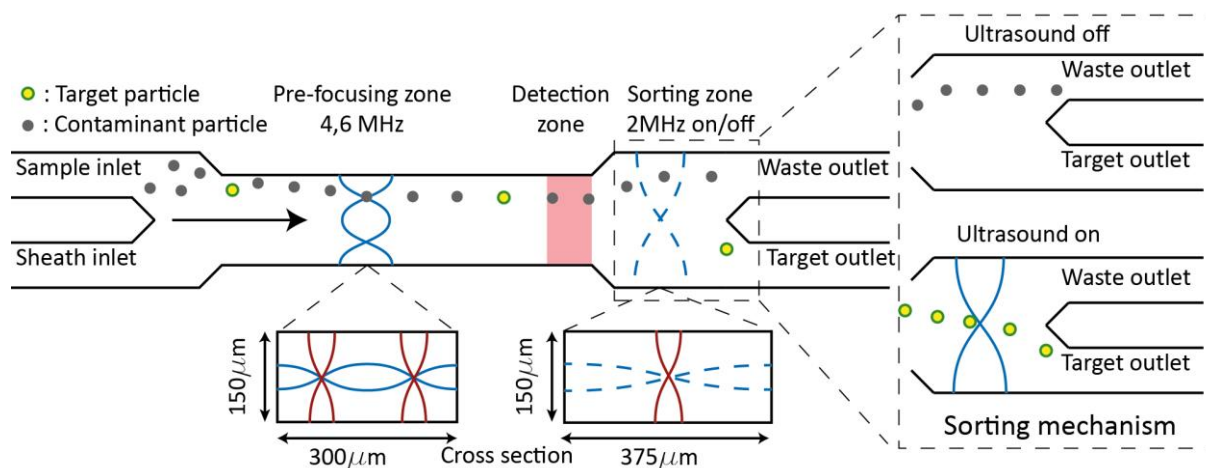
Figure 2. Schematic of the operating principle of the AFACS

An image of the AFACS-microchip used for the experiments is presented in Figure 3**,** showing the sample and sheet flow inlet (insert upper left) and the waste and target outlet (insert lower right). The two piezo electric actuators are seen glued to the back side of the chip where the long rectangular transducer operates the 2-dimensional pre-focusing zone and the smaller square transducer drives the sorting zone. The total length of the chip is 45 mm.
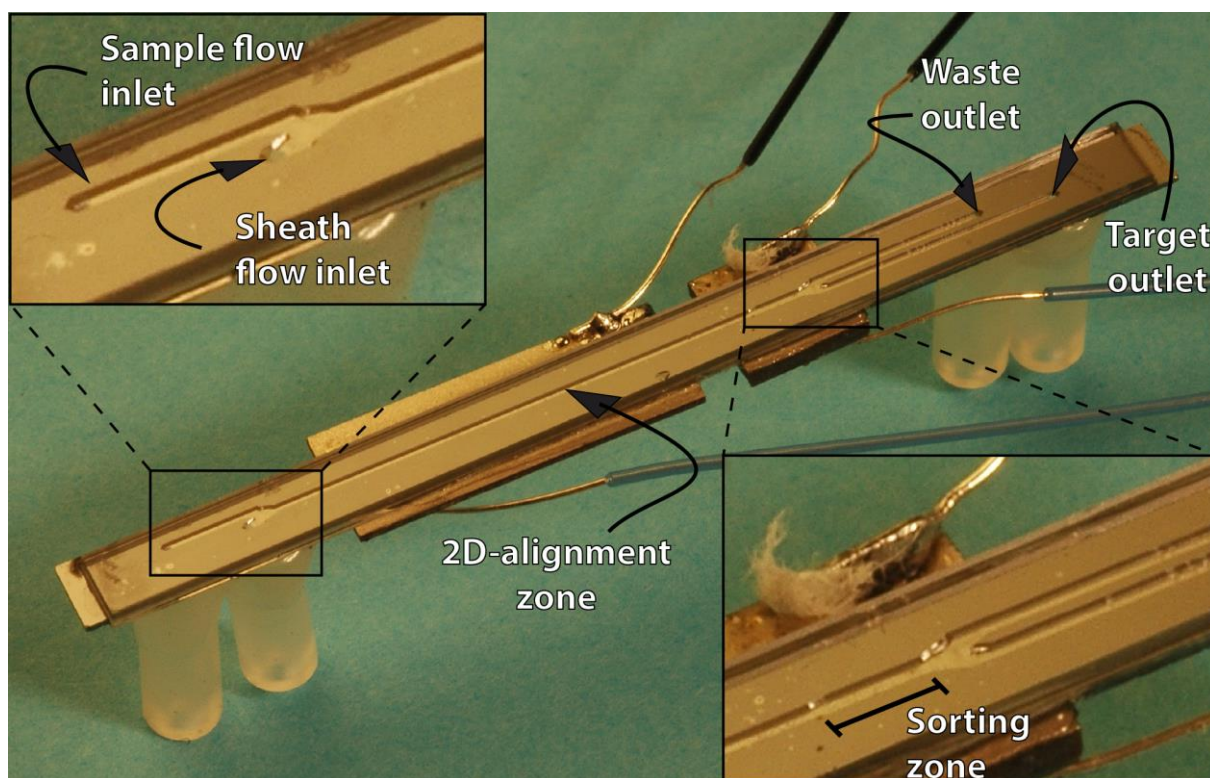
Figure 3. A photograph of the AFACS-microchip. The inserts show close-ups of the inlet and outlet of the chip.

Results and Discussion

Characterization of the two-dimensional pre-focusing

The two-dimensional pre-focusing is essential for the AFACS in 3 ways:

1. Positioning all particles into the same flow vector, resulting in uniform velocities and retention times within the system.
2. Positioning the particles where the acoustic radiation force is at its maximum when performing the acoustophoretic particle switching, thus minimizing the acoustic actuation time for deflection of pre-aligned particles.
3. Positioning the particles in the focal plane of the detector, improving detection performance.

The two-dimensional focusing was experimentally verified using confocal microscopy, as shown in Figure 4. At flow rates above 2 mL min^{-1}, the retention time in the pre-focusing zone was not sufficient at the given acoustic force to focus particles two-dimensionally into a well defined and confined stream line.
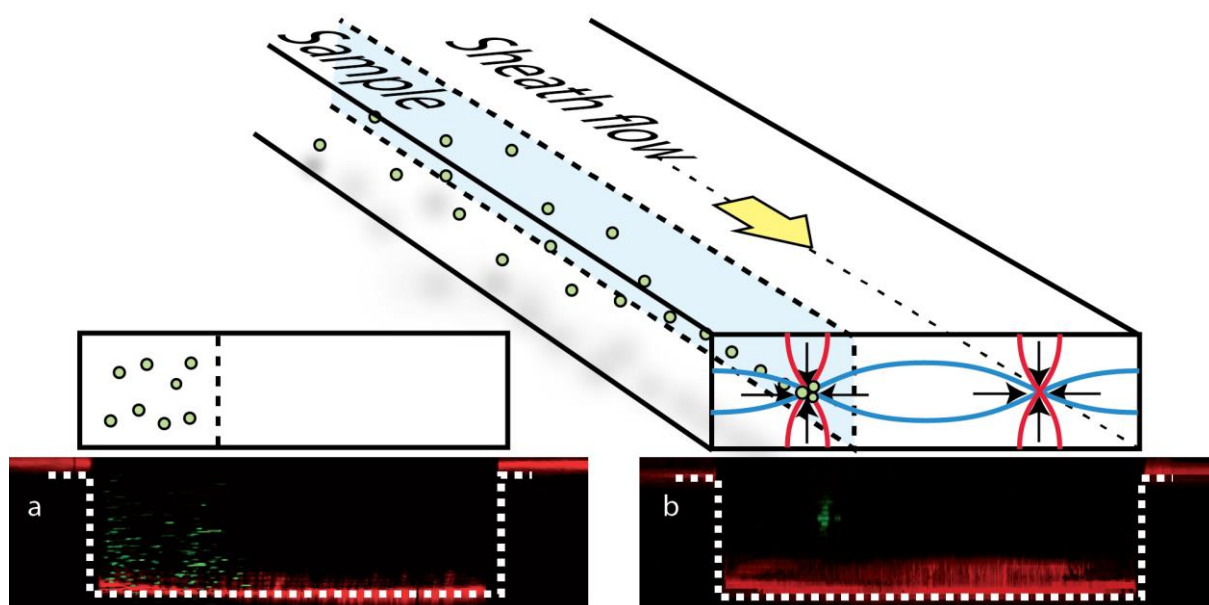
Figure 4a. A confocal image projection of the cross-section of the pre-focusing zone, showing unfocused FITC marked polystyrene beads at 300 µL min^{-1}. The red color (and the dashed line) indicates the chip boundary. **b:** A confocal image projection of the cross-section of the acoustic FACS micro-channel, showing two-dimensional acoustic pre-focusing of FITC marked polystyrene beads at a flow rate of 300 µL min^{-1}.

To illustrate the effect of the two acoustic actuation modes, Figure 5a-d shows an image sequence of the particle trajectories in the sorting zone. In Figure 5b the pre-focusing is inactivate, in Figure 5c pre-focusing has been activated and in Figure 5d, both pre-focusing and sorting actuation has been activated in continuous mode. It can be noted that the retention time of the particles in the sorting zone is well within the time window to be translated into the channel centre before exiting the chip.
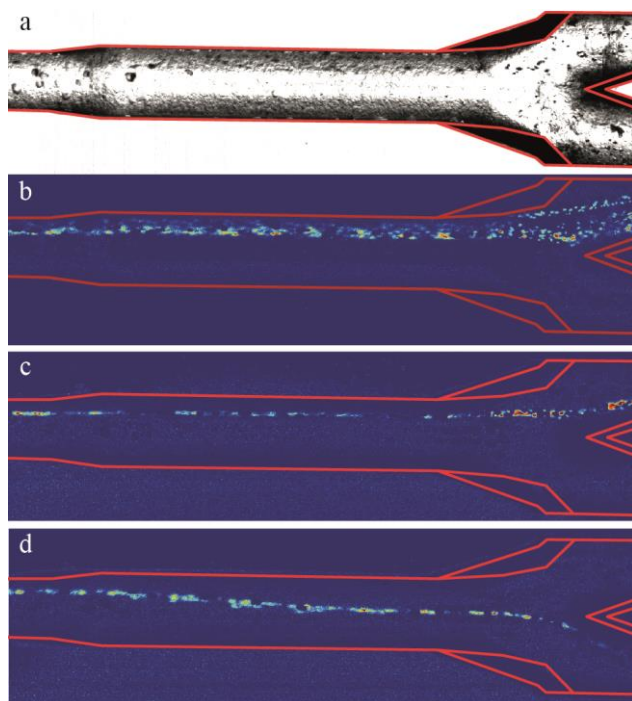
Figure 5a: A bright field image showing the sorting zone of the microfluidic chip. The walls of the chip are outlined in red. The direction of flow is from left to right. The lower outlet is the target outlet.

b: Image of the sorting zone where particles are visualized using background subtraction. No actuation of the 2-D pre-focusing is employed, showing particles distributed across the entire sheet flow region along the top most side wall

c: Pre-focusing zone is actuated, showing particles focused into a confined stream approximately 90μm out from the top most side wall. The sorting transducer is not activated. Particles are recovered in the waste outlet (top outlet).

d: Pre-focusing and sorting zone is actuated simultaneously. Particles are recovered in the target outlet (lower outlet)

The retention time for a particle in the sorting zone is critical as this parameter sets the limit of the system throughput and the highest possible flow rate is desired in this respect. For optimal system performance the input power and duration of the acoustic sorting burst signal should be matched to the retention time, see S1 of SI. For this reason, the velocity of the particles in the two dimensional focusing position was measured in the "sorting zone" for a varying set of flow rates. The measured velocity increased linearly with the flow rate and the relative standard deviation of the particle velocity distribution was less than 10% at a flow rate of 2mL/min, see S2 of SI.

Characterization of switching time

To find the minimum acoustic burst time necessary for deflecting a particle sufficiently to be translated into the target outlet, a highly concentrated particle suspension with 10 μm polystyrene beads was injected into the chip. The 2 MHz transducer was actuated periodically with a 10 % duty cycle, and the burst length was reduced until particles were no longer translated into the target outlet. The sorting zone and the two outlets of the chip were monitored by a high-speed camera, capturing images at approximately 6000 frames per second. The minimum acoustic burst time required to deflect particles sufficiently for capture in the target outlet was found to be 500 μs (1000 periods at 2 MHz). Figure 6 shows a time-lapse sequence of an acoustic burst lasting 1 ms. A video demonstrating 100Hz periodic gating with a 10% gating duty cycle (1ms) is available in S4 of SI.
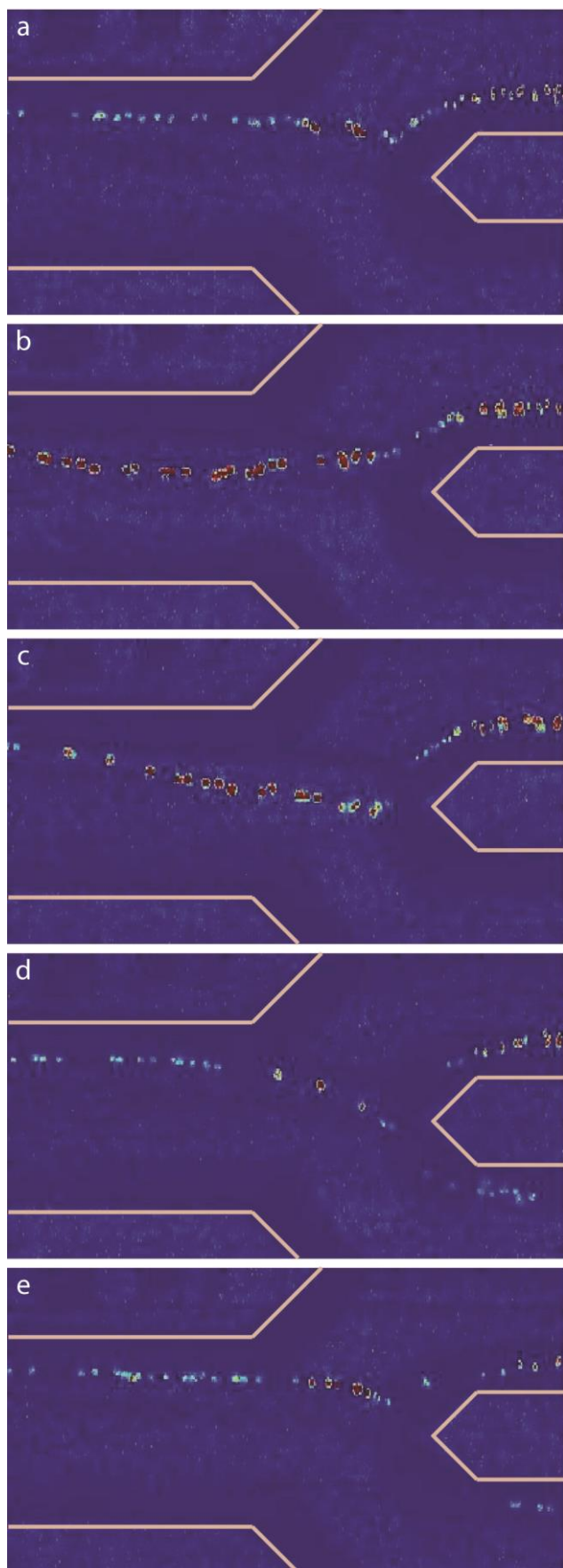
Figure 6a: t=0ms The ultrasound is turned on. **b**: t=1ms The ultrasound is turned off. Particles are deflected towards the center of the sorting zone, upstream of the flow splitter. **c**: t=1.6ms The deflected particle stream is breaking of from the non-actuated particle segment, approaching the flow splitter towards the sorting outlet. **d**: t= 2.5ms Deflected particles exit through the target outlet. **d**: t=3.3ms. Particles are again exiting through the waste outlet. The last few particles that were deflected are still seen exiting the sorting outlet

Sorting performance

The samples were injected into the chip at 200 µl min^{-1}. The acoustic burst time was set to 2.5, 4, or 8 ms. The number and times of triggering events were continuously sampled. As the system lacked the equivalent to a forward scatter signal, the total throughput in particles s^{-1} had to be estimated:

$$throughput = \frac{triggering\ events/s}{starting\ purity}$$

As the detector could not distinguish between positive events close to each other, the throughput was most likely underestimated. At least 10000 particles were sorted per experiment. Experimental parameters are given in table 1.

Acoustic actuation time (ms)/burst	4.6 MHz Sine V$_{pp}$ (continuous)	2.0MHz Sine V$_{pp}$ (burst)	Sample flow rate (µL/min)	Sheath flow rate (µL/min)	Average particles/s
6	3	30	200	600	50, 100, 150
4	3	30	200	1100	50, 100, 150
2.5	4	40	200	1500	50, 100, 150

Table 1. Experimental parameters for each experiment.

The sample flow rate was deliberately kept constant at 200 µL min^{-1} to reduce experimental variations due to sedimentation effects in syringes and sample inlet tubing. The obtained purity as a function of the acoustic actuation time of the sorting zone and throughput is seen in Figure 7. The average recovery of target particles for all experiments was 93.2 ± 2.6 %. The device did not show any sign of clogging during any experiment.
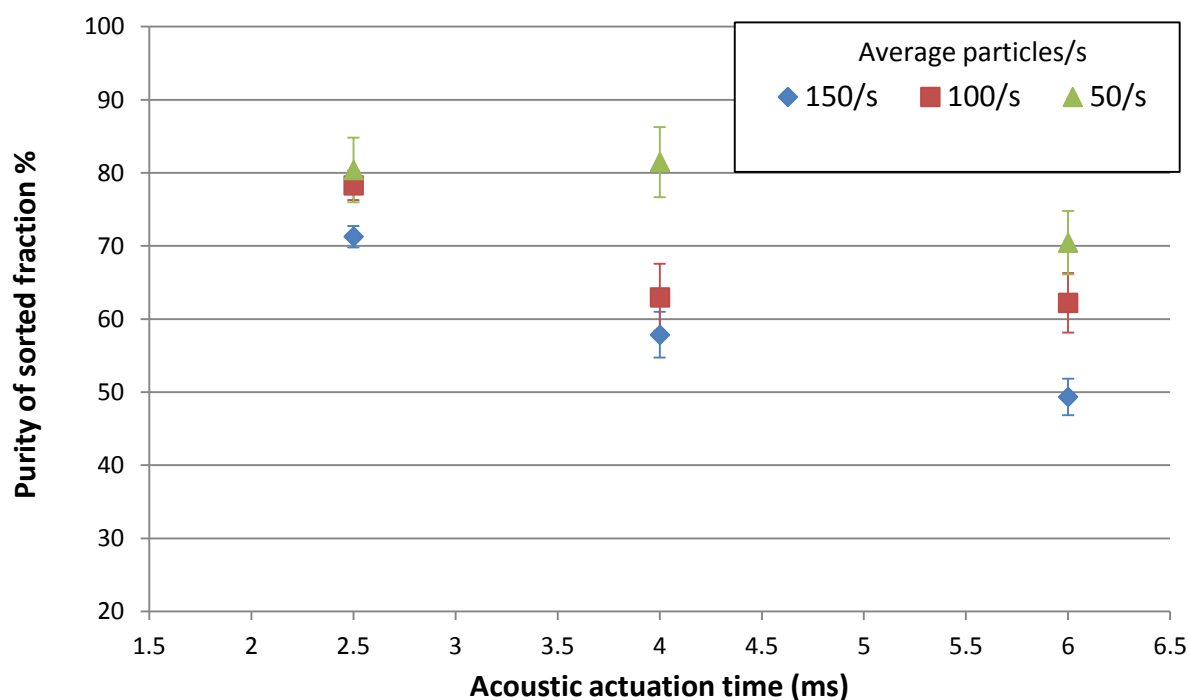
Figure 7. Sorting performance for 34 experiments with different throughput and acoustic actuation time. The purity of the sample injected into the chip was 19.5 %. Each data point is an average of either three or four experiments. The standard deviation is shown by the error bars.

### The relation between purity and throughput

The primary factor affecting the sort purity is the relation μ between the "acoustic actuation time" and the average time between events (throughput) in the channel

$$\mu = \frac{Acoustic\ actuation\ time}{average\ time\ between\ events}$$

The expected purity for an experiment is calculated by using probability theory, assuming the system works ideally and a Poisson distributed event rate (See S3 of SI):

$$Minimum\ expected\ purity = \frac{1}{1+\mu}$$

As the acoustic burst time is decreased, the probability of capturing more than one particle is reduced, thus increasing the purity. Reducing the particle concentration, but maintaining the total flow rate will result in more space between the particles and does also decrease the probability of capturing false positives. Figure 8 shows experimental data for the relation between purity and μ, together with a calculated (expected purity) line. Most data points fall below the theoretical value. This might be caused by trigger timing errors, an underestimated μ value (throughput or acoustic burst time), or a non-Poisson distributed sample (eg. sample aggregation or sample flow variations). In theory, it should be hard to obtain sort purities above this theoretical line. To the best of our knowledge, this limitation applies to all continuous flow based sorters that lack the equivalent to a "coincidence abort"[7] function.
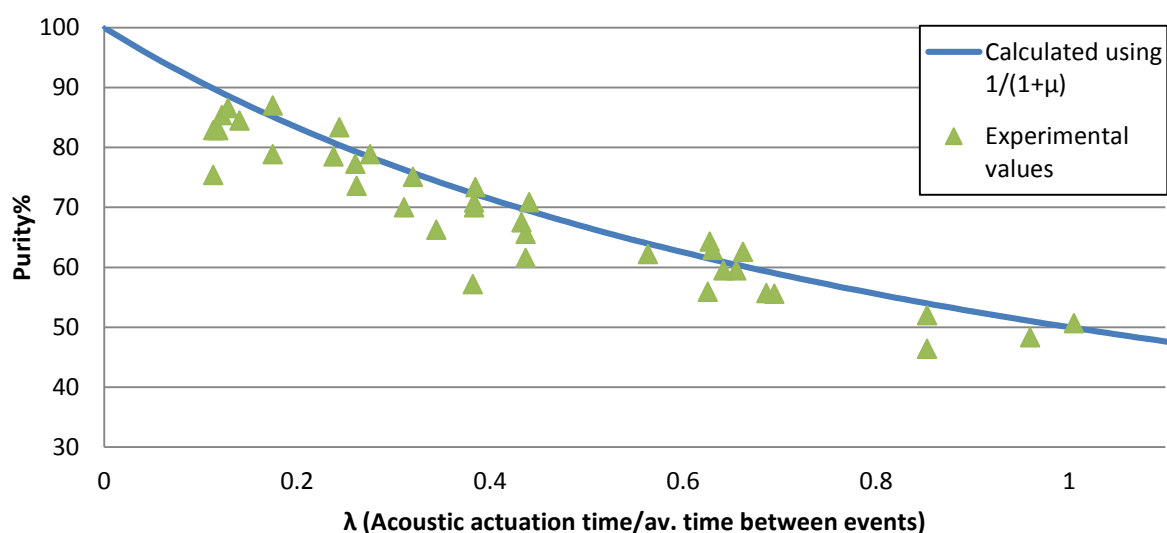
Figure 8. Purity vs μ for 36 experiments. The blue line shows the calculated expected minimum purity.

Future improvements and outlook

Integration of a forward scatter signal detector (FSC) would allow the AFACS system to detect non-fluorescent particles in the sorting zone, giving it the ability to sort with a much higher purity by implementing the equivalent to a "sort mask" (coincidence abort function) when making a sorting decision.

Shortening of the "sorting zone" would allow a shorter acoustic actuation time, increasing performance of the system. Experiments showed that an acoustic actuation time of 500 μs was sufficient to deflect particles for recovery in the target outlet. However, due to the required 1:1 relation between particle retention time in the sorting zone and acoustic actuation time, using such a short acoustic burst would require a total flow rate of approximately 8 mL min^{-1}. The current limitation of the "pre-focusing zone" was, however, about 2 mL min^{-1} for the microchip used, but this could be alleviated by a longer "pre-focusing zone".

Since the acoustic force on a particle scales with the volume, sorting of smaller particles would be less efficient in the present system. However this can be addressed by suspending the sample in a fluid with a higher density compared to the sheath fluid, allowing the ultrasound to act on the entire sample stream rather than the individual particles, similar to the method demonstrated by Johansson et al [6].

By realizing a sorter in continuous flow, as opposite to two-phase flow[27, 28] or aerosol-based techniques (drop in air), the option of integrating additional functionality (such as a second sorter) downstream or parallel of the sorter becomes available. The acoustic two-dimensional focusing gives a large flexibility in terms of sample to sheath flow ratio, and a recent study has shown that acoustic focusing can be utilized to achieve sheath-less parallel flow cytometry[11]. As the smallest dimension at any point in the device is 150μm and the deflection distance for a sort event is ~90μm, the device may also be suitable for sorting of larger entities such as clusters of cells or ovum cells. The dimensions of the chip in combination with the high flow rates used in the experiments made the system very resistant to clogging, and no sample pretreatment (filtering) was needed.

When comparing the performance of the AFACS to other FACS systems, both the purity and the throughput must be taken into consideration. E.g. very high throughputs can be obtained by doing very low purity sorts[29]. The performance of a FACS system should not be measured as an enrichment number, as this parameter is sample-dependent. We have shown that the limiting factor for our system, and to the best of the authors' knowledge, for all continuous flow based FACS systems, is how long time the sample stream is deflected during a sort event (denoted as t_sort in S3 of S1). It is also shown that this variable links throughput and purity together, and we propose that the performance of a FACS system should be measured using this variable.

Conclusion

We have showed that acoustic standing wave forces can be used to achieve Lab-on-a-chip integrated FACS sorting in a continuous flow. Although slower than most commercially available FACS systems, the benefits of a closed sample line and a continuous flow system with possibility of integration with additional downstream microfluidic unit operations, may outweigh the drawbacks of a reduced throughput.

References

1. J. F. Leary, in *Current Protocols in Cytometry*, John Wiley & Sons, Inc., 2001.
2. A. Y. Fu, C. Spence, A. Scherer, F. H. Arnold and S. R. Quake, *Nature Biotechnology*, 1999, **17**, 1109-1111.
3. S. Fiedler, S. G. Shirley, T. Schnelle and G. Fuhr, *Analytical Chemistry*, 1998, **70**, 1909-1915.
4. M. M. Wang, E. Tu, D. E. Raymond, J. M. Yang, H. Zhang, N. Hagen, B. Dees, E. M. Mercer, A. H. Forster, I. Kariv, P. J. Marchand and W. F. Butler, *Nat Biotech*, 2005, **23**, 83-87.
5. S. H. Cho, C. H. Chen, F. S. Tsai, J. M. Godin and Y.-H. Lo, *Lab on a Chip*, 2010, **10**, 1567-1573.
6. L. Johansson, F. Nikolajeff, S. Johansson and S. Thorslund, *Analytical Chemistry*, 2009, **81**, 5188-5196.
7. H. M. Shapiro, *Practical flow cytometry, Third edition*, Wiley-Liss, Inc., 605 Third Avenue, New York, New York 10158-0012, USA Chichester, England, 1995.
8. *Flow Cytometry for Biotechnology*, Oxford Univ Press, 198 Madison Avenue, New York, Ny 10016 USA, 2005.
9. L. P. Gorkov, *Doklady Akademii Nauk Sssr*, 1961, **140**, 88-&.
10. A. Nilsson, F. Petersson, H. Jonsson and T. Laurell, *Lab on a Chip*, 2004, **4**, 131-135.
11. M. E. Piyasena, P. P. A. Suthanthiraraj, R. W. Applegate, A. M. Goumas, T. A. Woods, G. P. Lopez and S. W. Graves, *Analytical Chemistry*, 2012, **84**, 1831-1839.
12. M. Nordin and T. Laurell, *Lab on a Chip*, 2012, **12**, 4610-4616.
13. F. Petersson, L. Aberg, A. M. Sward-Nilsson and T. Laurell, *Analytical Chemistry*, 2007, **79**, 5117-5123.
14. P. Augustsson, C. Magnusson, M. Nordin, H. Lilja and T. Laurell, *Analytical Chemistry*, 2012, **84**, 7954-7962.
15. T. Franke, S. Braunmuller, L. Schmid, A. Wixforth and D. A. Weitz, *Lab on a Chip*, 2010, **10**, 789-794.
16. X. Ding, S.-C. S. Lin, M. I. Lapsley, S. Li, X. Guo, C. Y. Chan, I. K. Chiang, L. Wang, J. P. McCoy and T. J. Huang, *Lab on a Chip*, 2012, **12**, 4228-4231.
17. M. A. Burguillos, C. Magnusson, M. Nordin, A. Lenshof, P. Augustsson, M. J. Hansson, E. Elmer, H. Lilja, P. Brundin, T. Laurell and T. Deierborg, *Plos One*, 2013, **8**.
18. J. Dykes, A. Lenshof, I. B. Astrand-Grundstrom, T. Laurell and S. Scheding, *Plos One*, 2012, **7**, e30074.
19. C. Simonnet and A. Groisman, *Analytical Chemistry*, 2006, **78**, 5653-5663.
20. S. Choi, S. Song, C. Choi and J.-K. Park, *Small*, 2008, **4**, 634-641.
21. A. J. Chung, D. R. Gossett and D. Di Carlo, *Small*, 2013, **9**, 685-690.
22. D. Holmes, H. Morgan and N. G. Green, *Biosensors & Bioelectronics*, 2006, **21**, 1621-1630.
23. X. Mao, A. A. Nawaz, S.-C. S. Lin, M. I. Lapsley, Y. Zhao, J. P. McCoy, W. S. El-Deiry and T. J. Huang, *Biomicrofluidics*, 2012, **6**.
24. M. Piagnerelli, K. Z. Boudjeltia, D. Brohee, A. Vereerstraeten, P. Piro, J. L. Vincent and M. Vanhaeverbeek, *Journal of Clinical Pathology*, 2007, **60**, 549-554.
25. G. Goddard, J. C. Martin, S. W. Graves and G. Kaduchak, *Cytometry Part A*, 2006, **69A**, 66-74.
26. O. Manneberg, J. Svennebring, H. M. Hertz and M. Wiklund, *Journal of Micromechanics and Microengineering*, 2008, **18**.
27. J.-C. Baret, O. J. Miller, V. Taly, M. Ryckelynck, A. El-Harrak, L. Frenz, C. Rick, M. L. Samuels, J. B. Hutchison, J. J. Agresti, D. R. Link, D. A. Weitz and A. D. Griffiths, *Lab on a Chip*, 2009, **9**, 1850-1858.
28. C. Lee, J. Lee, H. H. Kim, S.-Y. Teh, A. Lee, I.-Y. Chung, J. Y. Park and K. K. Shung, *Lab on a Chip*, 2012, **12**, 2736-2742.
29. A. Wolff, I. R. Perch-Nielsen, U. D. Larsen, P. Friis, G. Goranovic, C. R. Poulsen, J. P. Kutter and P. Telleman, *Lab on a Chip*, 2003, **3**, 22-27.